Available online at www.sciencedirect.com
SCIENCE DIRECT®
Journal of Power Sources 119–121 (2003) 145–149
JOURNAL OF POWER SOURCES
www.elsevier.com/locate/jpowsour

A study of layered lithium manganese oxide cathode materials

Tom A. Eriksson, Marca M. Doeff*

Materials Sciences Division, Lawrence Berkeley National Laboratory, University of California at Berkeley, Berkeley, CA 94720, USA

Abstract

Substituted layered sodium manganese oxide bronzes with the P2 structure were prepared by glycine-nitrate combustion synthesis. The Na in the *as-prepared* materials could be completely ion-exchanged for Li under mild conditions. All lithium manganese oxide compounds obtained after ion-exchange have O2 stacking of the layers. Cyclic voltammetry and stepped potential experiments on lithium cells containing these materials show that the main redox reaction around 3.1 V is a diffusion-controlled process and is completely reversible. O2-$Li_{0.6}[Al_{0.1}Mn_{0.85}\square_{0.05}]O_2$ and O2-$Li_{0.6}[Ni_{0.1}Mn_{0.85}\square_{0.05}]O_2$ are particularly promising as cathode materials in lithium cells because of the high reversible discharge capacities (180 mAh/g).

Keywords: Cathode; Lithium battery; Manganese oxide

1. Introduction

Novel materials for use as electrodes in Li-ion batteries have attracted much attention since Sony produced the first commercial Li-ion batteries in 1990 [1,2]. Commercial Li-ion battery electrodes today contain expensive and hazardous compounds, like lithium cobalt or nickel oxides or combinations of these. It is desirable to replace these with a manganese-based system, which is potentially cheaper and less toxic. However, the 3D spinel structures of lithium manganese oxides exhibit low capacities and poor cycling behavior. Recently layered lithium manganese oxides have been investigated in an attempt to improve these properties [3,4]. $LiMnO_2$ with the α-$NaMnO_2$ structure, however, transforms into the more stable spinel structure upon electrochemical cycling. A non-stoichiometric layered sodium manganese oxide, $Na_{0.7}MnO_{2+y}$, with a stacking sequence different from α-$NaMnO_2$, can be ion-exchanged to produce an electrode that should not transform into spinel upon cycling [5]. When directly synthesized with Na as the alkali metal ion the materials have a P2 structure, where P indicates a prismatic oxygen environment for the alkali metal ion and 2 indicates the number of MO_2 sheets within the unit cell. Upon ion-exchange, the stacking of the layers changes to O2 or O6 where the Li-ion is in an octahedral site, or to T2 where the Li-ion is in a tetrahedral site [6]. These materials showed promising electrochemical behavior, with a high initial discharge capacity. However, samples in the previous studies were incompletely exchanged, complicating interpretation of the cell cycling behavior.

Materials in the earlier studies had fairly large particle sizes (above 10 μm) [7]. We have used glycine-nitrate combustion synthesis to produce the precursor P2-$Na_{0.7}M_xMn_{1-x}O_2$ (where M is a metal substituent) compounds [8,9]. This method produces small particles that are more easily ion-exchanged under mild conditions than larger particles produced by conventional solid-state synthesis. The milder ion-exchange has proven to be the most effective way to obtain stable cycling in layered lithium manganese oxide electrode materials [10,11]. Additionally, partial substitution of manganese has been observed to improve their cycling behavior.

2. Experimental

2.1. Synthesis

The desired proportions of $NaNO_3$, 47.5% $Mn(NO_3)_2$ in HNO_3 and substituent metal-nitrate ($Ni(NO_3)_3{\cdot}6H_2O$ or $Al(NO_3)_3{\cdot}9H_2O$) were mixed with glycine in the molar ratio 1:2 (glycine:nitrate) and diluted with de-ionized water. The temperature of the combustion reaction is determined by the glycine:nitrate ratio and was chosen to give 1300–1400 °C [8]. The solution was mixed with a magnetic stirrer over night, until all the nitrates were dissolved, and then slowly dripped into a metal beaker placed on a hot plate. The water evaporated and the nitrates reacted exothermically, with the

* Corresponding author. Tel.: +1-510-486-5821; fax: +1-510-486-4881.
E-mail address: mmdoeff@lbl.gov (M.M. Doeff).

0378-7753/03/$ – see front matter
doi:10.1016/S0378-7753(03)00144-7

glycine acting as fuel for the reaction. The *as prepared* powder was calcined at 800 °C for 4 h to remove any organic residue and to obtain a homogenous material.

The materials were refluxed in a solution of LiBr in ethanol (nine-fold excess of Li) for 48 h at 80 °C, for the ion-exchange.

2.2. Electrode preparation and cell assembly

The electrodes were prepared by thoroughly mixing 80 wt.% active material with 6% carbon black (Shawinigan Black), 6% SFG-6 graphite (Timrex Timcal) and 8% PVdF (from a 6% NMP-solution) and extruding onto an aluminum-foil. The electrodes were allowed to dry over night at room temperature and for 24 h at 120 °C. Coin cells were assembled in a glove-box (<1 ppm O_2/H_2O) using Cellgard 3401 as separator, ethylene-carbonate (EC)/dimethyl-carbonate (DMC) + 1 M $LiPF_6$ electrolyte (Selectipur®, Merck, Darmstadt, Germany), and Li-foil (Cyprus-Foote Mineral Co., Kings Mountain, NC) as the counter electrode.

2.3. Analysis

X-ray diffraction (XRD) was performed on a Siemens 5000D diffractometer, with monochromized Cu radiation ($\lambda = 1.54$ Å). Scanning electron microscopy (SEM) was performed on a Microspec ISI-DS 130C microscope. An Arbin BT/HSP-2043 was used for the cyclic voltammetry (CV) experiments. Potential limits were set to 4.3 and 2.0 V. For the potential step measurements, a MacPile II (Bio-Logic, SA, Claix, France) was used. The elemental composition was determined by inductively coupled plasma (ICP) analysis (by Desert Analytics Laboratory, Tucson, AZ).

3. Results and discussion

The chemical analysis of the sodium-containing precursors yields a molar ratio of 0.6Na:0.1M:0.85Mn (where M = Al or Ni). This is consistent with density measurements performed by Parant et al. indicating vacancies are present in hexagonal P2 phases [12]. The composition can thus be written as $Na_{0.6}[M_{0.1}Mn_{0.85}\square_{0.05}]O_2$. After ion-exchange, ICP shows that the material has less than 7% sodium in the structure and the lithium content is about $x = 0.56$. No traces of the sodium P2 phase can be seen by XRD, implying that the sodium residue, seen with ICP, may be from sodium-containing impurities on the surface or to a small amount of sodium between the layers. By analogy to the sodium-containing precursors, we refer to the lithiated compounds as $Li_{0.6}[Al_{0.1}Mn_{0.85}\square_{0.05}]O_2$ or $Li_{0.6}[Ni_{0.1}Mn_{0.85}\square_{0.05}]O_2$ in this work.

From the XRD measurements, it can be concluded that the lithiated materials have primarily the O2 structure, with the peak assignments shown in Fig. 1. No evidence of the T2 structure could be found in any samples (the T2 phase

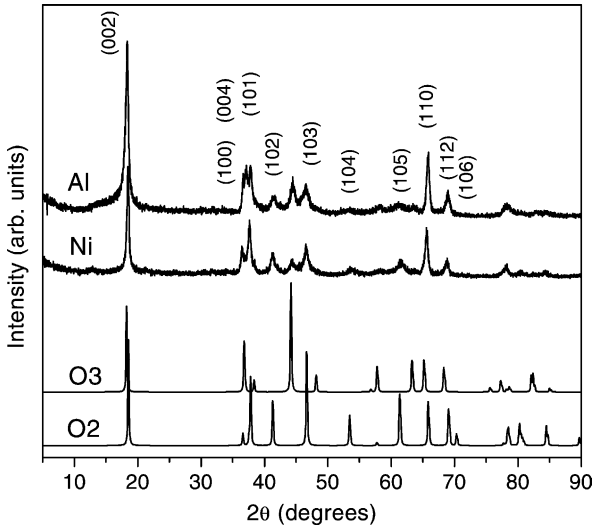

Fig. 1. XRD patterns of $Li_{0.6}[Al_{0.1}Mn_{0.85}\square_{0.05}]O_2$ and $Li_{0.6}[Ni_{0.1}Mn_{0.85}\square_{0.05}]O_2$. The theoretical XRD patterns of rhombohedral O3 and hexagonal O2 structures are also included.

should appear as a split in the (1 1 0) peak at 66° in 2θ [6]). Small peaks matching the strongest reflection from a rhombohedral O3 structure (1 0 3) can also be observed. In the patterns of the sodium containing precursors, several weak peaks at moderate and high angles were present which could not be indexed to the hexagonal P2 structure or to an α-$NaMnO_2$ type structure (monoclinic, with O3 stacking), which may form in sodium-rich mixtures [12,13] (significantly, no extra peak at low angles was observed). These are, however, consistent with the presence of small amounts of an undistorted $R\bar{3}M$ phase with O3 stacking, analogous to non-stoichiometric $Na_xMn_yO_2$ phases prepared at low temperatures by Armstrong et al. [14]. It is not yet clear whether this exists as a separate phase or as an intergrowth with the P2 structure (i.e. stacking faults). Upon ion-exchange, a non-stoichiometric rhombohedral O3-$Li_xMn_yO_2$ is formed, as is seen in Fig. 1.

As can be seen in the diffractograms, the peak-shape and intensity varies between different reflections (Fig. 1). For instance, the (0 0 2) and (1 1 0) reflections are very sharp and narrow with high intensities, while most of the other reflections are rather broad and not clearly defined. This is especially prominent for the (h 0 l) reflections. This indicates the presence of stacking faults (or, alternatively, residual sodium between layers), and makes Rietveld refinement of these patterns difficult to carry out with acceptable statistics. Because sliding of the MnO_2 layers, which occurs during ion-exchange and conversion of the P2 sodium form, can result in a number of different stackings, there is a high probability of ending up with a mix of, e.g. O2, O6, and T2 stackings [15]. ^{7}Li MAS NMR experiments and transmission electron microscopy (TEM) analysis are more sensitive probes of local environments and are currently being undertaken to better understand the nature of the faults in these layered materials [13].

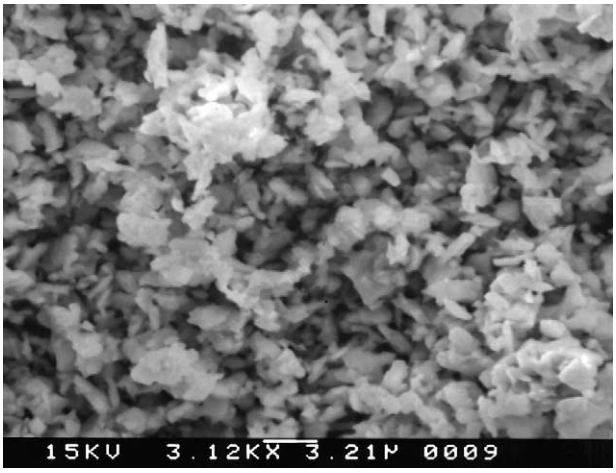

Fig. 2. SEM image of $Li_{0.6}[Ni_{0.1}Mn_{0.85}\square_{0.05}]O_2$.

The morphologies of the ion-exchanged powders were studied with SEM (Fig. 2). It was found that they consist of small crystallites, about 1–4 μm across, which are slightly fused together from the calcination, into larger agglomerates of 15–30 μm. These larger particles are very porous, allowing ready access of the electrolyte solution.

$Li/Li_{0.6}[Al_{0.1}Mn_{0.85}\square_{0.05}]O_2$ and $Li/Li_{0.6}[Ni_{0.1}Mn_{0.85}\square_{0.05}]O_2$ cells, as assembled, are in the partially discharged state and typically have OCPs of about 3.1–3.3 V. Cells may either be charged or discharged initially. Cyclic voltammetry experiments on $Li/Li_{0.6}[Al_{0.1}Mn_{0.85}\square_{0.05}]O_2$ cells show a highly reversible redox reaction (Fig. 3A). Only one distinct peak can be observed in both scan directions and the difference in oxidation and reduction potential is 0.39 V. This is unlike that of the differential capacity profiles previously reported for similar layered materials, which had main peaks near 3.0 V and one or two smaller peaks just below 4.0 V [16,17]. We have previously observed that electrochemical properties of cathode materials derived from sodium manganese oxides vary considerably with the degree of exchange [18]. The presence of sodium ions between the layers and/or variations in the type and amount of stacking faults in the materials reported on earlier may account for the observed differences. Significantly, no changes in the cyclic voltammograms of our cells were observed after five consecutive sweeps, indicating that conversion to spinel or to other phases does not occur under these conditions. This suggests that $Li_{0.6}[Al_{0.1}Mn_{0.85}\square_{0.05}]O_2$ should cycle stably in lithium or lithium ion configurations. Preliminary galvanostatic cycling experiments indicate no phase conversion occurs over more than thirty cycles, when the charge is limited to 4.2 V [13].

The $Li/Li_{0.6}[Ni_{0.1}Mn_{0.85}\square_{0.05}]O_2$ cell (Fig. 3B) shows one main peak in both scan directions although it is somewhat broader than for the Al-substituted compound, and the potential difference between oxidation and reduction of 1.00 V indicates a more sluggish redox reaction for this sample. A minor second peak, possibly attributable to Ni redox processes, is also observed.

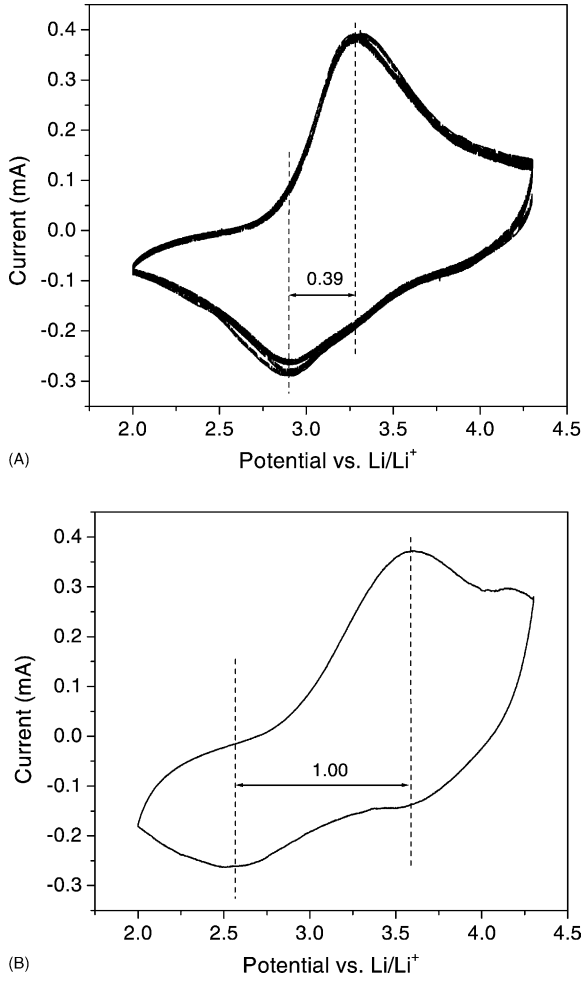

Fig. 3. Cyclic voltammetry experiments at a sweep rate of 0.05 mV/s: (A) 3 cycles on a charged $Li/Li_{0.6}[Al_{0.1}Mn_{0.85}\square_{0.05}]O_2$ cell, starting with the reduction sweep; (B) fourth cycle on a charged $Li/Li_{0.6}[Ni_{0.1}Mn_{0.85}\square_{0.05}]O_2$ cell.

Different sweep rates were used in order to investigate the nature of the redox reaction for $Li_{0.6}[Al_{0.1}Mn_{0.85}\square_{0.05}]O_2$ (Fig. 4). For diffusion-controlled reactions, the peak current is typically proportional to the square root of the sweep rate, whereas those without diffusion steps, e.g. reactions of surface species, are directly proportional to the sweep rate. Reactions involving the solutes or solvents of the electrolyte, i.e. electrolyte decomposition, should be of the diffusion-controlled type, even if the product is solid and remains at the surface (e.g. the solid electrolyte interface layer). It can be seen that there is a perfect linear relationship between the peak current and the square root of the sweep rate. Hence, the reactions in these electrode materials are diffusion controlled.

To obtain a pseudo open-circuit potential (OCP) profile, potential step experiments were performed. Differential capacity data obtained between 3.9 and 2.0 V was integrated to obtain the curves shown in Fig. 5A and B. The potential profiles are gradually sloping and do not show a distinct plateau. The midpoint potential is about 3.0 V and the capacity obtained between these voltage limits is 180 mAh/g for both

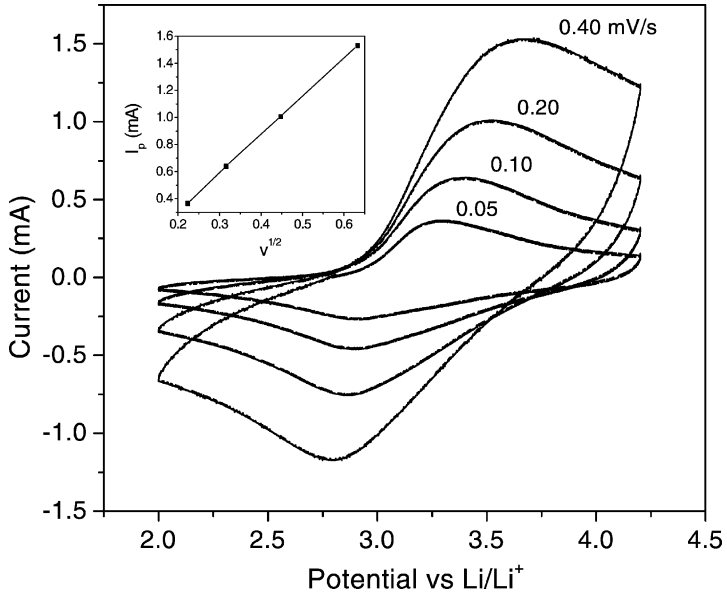

Fig. 4. Cyclic voltammetry experiments on a Li/$Li_{0.6}[Al_{0.1}Mn_{0.85}\square_{0.05}]O_2$ cell, at different sweep rates. Inset: the square-root of the sweep rate plotted against the peak current.

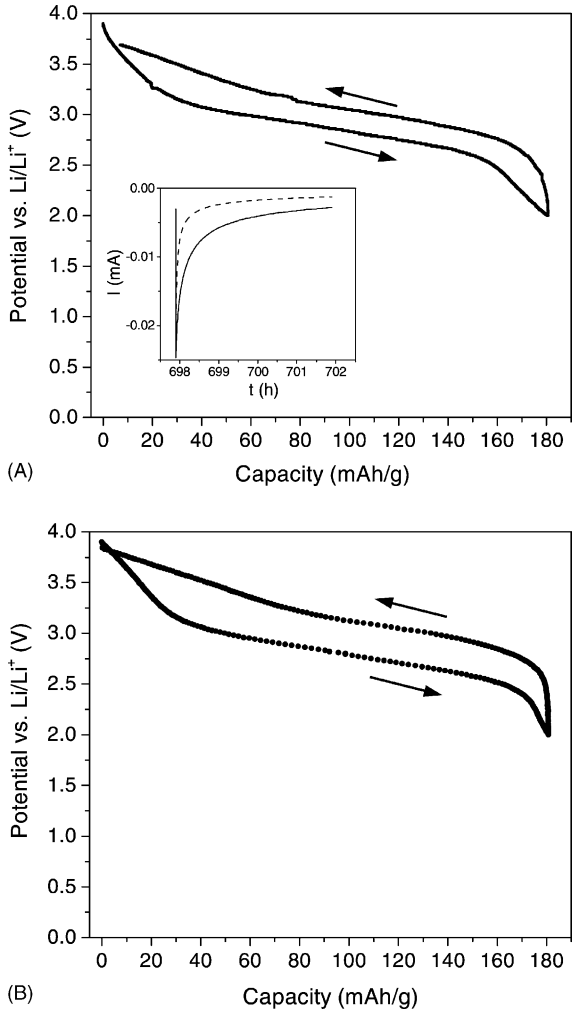

Fig. 5. Potential profiles from potential step measurements. A new step was taken every 4 h or when $I < 0.1$ μA: (A) Li/$Li_{0.6}[Al_{0.1}Mn_{0.85}\square_{0.05}]O_2$ cell. Inset: the *I–t* profile for one potential step at 2.90 V. The dotted line in the inset is a simulation of the Cottrell equation, offset for clarity; (B) Li/$Li_{0.6}[Ni_{0.1}Mn_{0.85}\square_{0.05}]O_2$ cell.

materials. $Li_{0.6}[Ni_{0.1}Mn_{0.85}\square_{0.05}]O_2$ shows a larger polarization than $Li_{0.6}[Al_{0.1}Mn_{0.85}\square_{0.05}]O_2$, confirming the CV results that insertion processes into this nickel-substituted sample are slower. More information on the nature of the redox reaction can be obtained by examining the I versus t behavior for potential steps in the region of interest. For processes controlled by diffusion (e.g. a single-phase reaction involving lithium insertion/de-insertion into a host), the current will increase or decrease proportionally with $t^{-1/2}$ at short times ($t \ll L^2/D$, where L is the diffusion path length and D is the chemical diffusion coefficient), according to the Cottrell equation [19]. This is seen for steps near 2.9 V in the discharge for the $Li_{0.6}[Al_{0.1}Mn_{0.85}\square_{0.05}]O_2$ cell (see inset in Fig. 5A), suggesting that the reaction is single-phase in this region. Galvanostatic cycling experiments on cells containing substituted layered lithium manganese oxides are presently underway in this laboratory and will be discussed in subsequent publications.

4. Conclusions

O2-$Li_{0.6}[Al_{0.1}Mn_{0.85}\square_{0.05}]O_2$ and O2-$Li_{0.6}[Ni_{0.1}Mn_{0.85}\square_{0.05}]O_2$ compounds may be used as cathodes in rechargeable lithium cells. Fully-exchanged materials prepared from P2 sodium manganese oxides precursors obtained via glycine-nitrate combustion synthesis appear to cycle stably and have attractive electrochemical properties, giving up to 180 mAh/g at an average potential of 3.0 V.

Acknowledgements

This work was supported by the Assistant Secretary for Energy Efficiency and Renewable Energy, Office of FreedomCAR and Vehicle Technologies of the US Department of Energy under Contract No. DE-AC03-76SF00098. T.A. Eriksson was funded by The Hans Werthen Foundation and The American–Scandinavian Foundation.

References

[1] M. Winter, J.O. Besenhard, M.E. Spahr, P. Novak, Adv. Mater. 10 (1998) 725.
[2] J.M. Tarascon, M. Armand, Nature 414 (2001) 359.
[3] A.R. Armstrong, P.G. Bruce, Nature 381 (1996) 499.
[4] B. Ammundsen, J. Paulsen, Adv. Mater. 13 (2001) 943.
[5] J.M. Paulsen, C.L. Thomas, J.R. Dahn, J. Electrochem. Soc. 146 (1999) 3560.
[6] J.M. Paulsen, R.A. Donaberger, J.R. Dahn, Chem. Mater. 12 (2000) 2257.
[7] J.M. Paulsen, D. Larcher, J.R. Dahn, J. Electrochem. Soc. 147 (2000) 2862.
[8] L.A. Chick, L.R. Pederson, G.D. Maupin, J.L. Bates, L.E. Thomas, G.J. Exarhos, Mater. Lett. 10 (1990) 6.
[9] L.R. Pederson, L.A. Chick, G.J. Exarhos, US Patent 5 114 702 (1992).
[10] A.D. Robertson, A.R. Armstrong, P.G. Bruce, J. Chem. Soc., Chem. Commun. (2000) 1997.
[11] A.D. Robertson, A.R. Armstrong, P.G. Bruce, Chem. Mater. 13 (2001) 2380.
[12] J.-P. Parant, R. Olazcuaga, M. Devalette, C. Fouassier, P. Hagenmuller, J. Solid State Chem. 3 (1971) 1.
[13] T.A. Eriksson, Y.J. Lee, J.A. Reimer, E.J. Cairns, M.M. Doeff, manuscript in preparation.
[14] A. Robert Armstrong, A.J. Paterson, A.D. Robertson, P.G. Bruce, Chem. Mater. 14 (2002) 710.
[15] Z. Lu, J.R. Dahn, Chem. Mater. 13 (2001) 2078.
[16] J.M. Paulsen, C.L. Thomas, J.R. Dahn, J. Electrochem. Soc. 147 (2000) 861.
[17] J.M. Paulsen, J.R. Dahn, J. Electrochem. Soc. 147 (2000) 2478.
[18] M.M. Doeff, T.J. Richardson, L. Kepley, J. Electrochem. Soc. 143 (1996) 2507.
[19] C.J. Wen, B.A. Boukamp, R.A. Huggins, J. Electrochem. Soc. 126 (1979) 2258.